

Deflagration with quantum and dipolar effects in a model of a molecular magnet

D. A. Garanin, Reem Jaafar

*Department of Physics and Astronomy, Lehman College, City University of New York,
250 Bedford Park Boulevard West, Bronx, New York 10468-1589, U.S.A.*

(Dated: 10 February 2010)

Combination of the thermal effect in magnetic deflagration with resonance spin tunneling controlled by the dipole-dipole interaction in molecular magnets leads to the increase of the deflagration speed in the *dipolar window* near tunneling resonances.

PACS numbers: 75.50.Xx, 75.45.+j, 76.20.+q

Molecular magnets such as Mn_{12}Ac , possessing an effective large spin $S=10$, are famous as mesoscopic systems demonstrating magnetic bistability due to the strong uniaxial anisotropy. Spectacular spin tunneling under the anisotropy barrier in molecular magnets was first seen in the steps in dynamical hysteresis curves.¹ The steps correspond to the values of the longitudinal magnetic field B_z at which the energy levels in both potential wells match. Here resonance spin tunneling leads to a faster relaxation responsible for a step of the magnetization. To the contrast, off resonance the main channel of relaxation is thermal activation over the top of the barrier. The difference between the two types of relaxation is shown in Fig. 1. In fact, spin tunneling requires a transverse field or any other term in the Hamiltonian that breaks the axial symmetry. Pure spin tunneling in the right panel in Fig. 1 requires that these terms be sufficiently strong, such as the transverse field of about 3 T in Mn_{12} . In the case of weaker tunneling interactions, the intermediate situation of a thermally assisted tunneling is realized. In this case spins tunnel after thermally mounting up to below the top of the barrier.²⁻⁵ The role of tunneling in the case of weaker tunneling interactions can be interpreted as some lowering of the barrier near resonances. For stronger tunneling interactions, the barrier is removed completely at resonances.

Tunneling and relaxation in molecular magnets can be described by the density matrix equation,² the most comprehensive account of which is given in Ref. 6. The latter numerically implements the universal spin-phonon interaction suggested in Refs. 7,8. This interaction is due to distortionless rotation of the crystal field acting on the spins by transverse phonons and it is completely expressed in terms of the crystal-field Hamiltonian \hat{H}_A without any unknown spin-lattice coupling constants.

Experiments of 2005 by Myriam Sarachik group showed the existence of propagating deflagration (burning) fronts in the molecular magnet Mn_{12}Ac that are similar to chemical burning.^{9,10} Javier Tejada group observed peaks in the deflagration speed on the bias magnetic field B_z that were interpreted as contribution of resonance spin tunneling.¹⁰ A detailed, mainly classical, theory of the magnetic deflagration including the ignition threshold and the accurate prefactor in the Arrhenius-type expression for the speed of the burning front was proposed in Ref. 11.

The physics of deflagration is based on triggering re-

laxation from a metastable state over potential barrier by the temperature increase as the result of relaxation accompanied by energy release. The burning front forms because the temperature in the regions still unburned (e.g., before the front) rises as the result of heat conduction from the hot areas where burning just occurred. The two main ingredients of deflagration thus are the Arrhenius dependence of the relaxation rate on temperature (making burning in the cold areas before the front negligibly slow) and heat conduction. Deflagration is mathematically described by the system of coupled i) rate equation for the number of particles (magnetic molecules) in the metastable state and ii) the heat conduction equation.

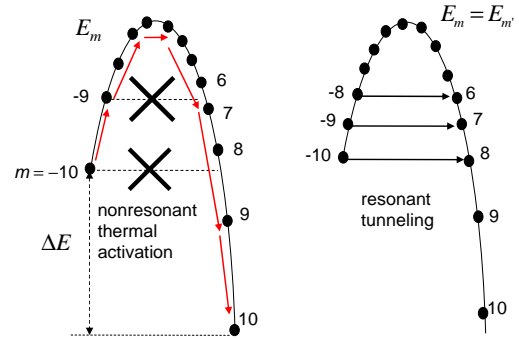


FIG. 1: Thermal activation in the nonresonant case vs tunneling in the resonant case.

Subsequent theoretical quest for an essentially quantum form of deflagration lead to the discovery of self-organized fronts of tunneling, a non-thermal process triggered by the dipolar field (rather than by temperature) that can bring the system on or off resonance.¹²⁻¹⁴ A hallmark of these fronts is the self-consistent adjustment of the metastable population (or magnetization) to the optimal spatial profile that creates the dipolar field that is constant in some region of space and brings the system on resonance. The width of the resonance region forming the front core is about the transverse dimension R of the sample that allows an efficient tunneling and thus front propagation. On the other hand, before and after the front core the system is off resonance and tunneling is blocked. Fronts of tunneling can be realized in the

dipolar window of the external field B_z

$$0 \leq B_z - B_k \leq B_z^{(D)}. \quad (1)$$

Here B_k is the field corresponding to the k th resonance in the absence of the dipolar field and $B_z^{(D)}$ is the dipolar field created by the uniformly magnetized elongated crystal. It was shown¹³ that the adjustment mechanism is robust with respect to resonance spread (e.g., due to defects) smaller than $B_z^{(D)}$.

The aim of the present paper is to unify the theories of the standard (hot) deflagration^{2,9} and fronts of tunneling (cold or quantum deflagration).^{13,14}

In the sequel we will use the generic model of a molecular magnet with $\hat{H}_A = -DS_z^2$, where the tunneling resonance fields are given by

$$B_k = kD / (g\mu_B), \quad k = 0, 1, \dots \quad (2)$$

Resonance tunneling occurs at $B_{\text{tot},z} = B_z + B_z^{(D)} \approx B_k$ between the metastable ground state $|-S\rangle$ and an excited state at the other side of the barrier $|m'\rangle$ with $m' = S - k$. At temperatures much smaller than the barrier height (e.g. at the temperature of the deflagration front) one can describe magnetic molecules as two-level systems occupying the states $|\pm S\rangle$. Let us denote the probability for a molecule to be in the metastable state $|-S\rangle$ as n . Then the average value of the effective pseudospin σ_z is

$$\sigma_z = 1 - 2n, \quad (3)$$

so that $n = 1$ corresponds to $\sigma_z = -1$. The general expression for the longitudinal component of the dipolar field on magnetic molecule i is the sum over positions of all other molecules j

$$B_{i,z}^{(D)} = \frac{Sg\mu_B}{v_0} D_{i,zz}, \quad D_{i,zz} \equiv \sum_j \phi_{ij} \sigma_{jz}. \quad (4)$$

Here v_0 is the unit-cell volume, D_{zz} is the reduced dipolar field, and

$$\phi_{ij} = v_0 \frac{3(\mathbf{e}_z \cdot \mathbf{n}_{ij})^2 - 1}{r_{ij}^3}, \quad \mathbf{n}_{ij} \equiv \frac{\mathbf{r}_{ij}}{r_{ij}}. \quad (5)$$

Inside a uniformly magnetized ellipsoid, $\sigma_z = \text{const}$, the dipolar field is uniform and one has $D_{zz} = \bar{D}_{zz} \sigma_z$, where

$$\bar{D}_{zz} = \bar{D}_{zz}^{(\text{sph})} + 4\pi\nu \left(1/3 - n^{(z)}\right), \quad (6)$$

ν is the number of magnetic molecules per unit cell ($\nu = 2$ for $\text{Mn}_{12} \text{Ac}$) and $n^{(z)} = 0, 1/3$, and 1 for a cylinder, sphere, and disc, respectively. The reduced dipolar field in a sphere $\bar{D}_{zz}^{(\text{sph})}$ depends on the lattice structure. For $\text{Mn}_{12} \text{Ac}$ lattice summation yields $\bar{D}_{zz}^{(\text{sph})} = 2.155$ that results in $\bar{D}_{zz}^{(\text{cyl})} = 10.53$ for a cylinder. Then Eq. (4) yields the dipolar field $B_z^{(D)} \simeq 52.6$ mT in an elongated sample that was also obtained experimentally.¹⁵

For simplicity we consider a long crystal of cylindrical shape of length L and radius R with the symmetry axis

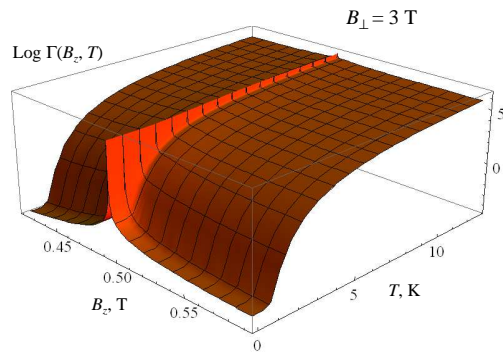


FIG. 2: Relaxation rate $\Gamma(B_z, T)$ in a generic model of a molecular magnet.

z along the easy axis, magnetized with $\sigma_z = \sigma_z(z)$. The latter assumption makes the problem tractable numerically. In this case the reduced magnetic field along the symmetry axis has the form¹²⁻¹⁴

$$D_{zz}(z) = \int_{-\infty}^{\infty} dz' \frac{2\pi\nu R^2 \sigma_z(z')}{\left[(z' - z)^2 + R^2\right]^{3/2}} - k\sigma_z(z), \quad (7)$$

where

$$k \equiv 8\pi\nu/3 - \bar{D}_{zz}^{(\text{sph})} = 4\pi\nu - \bar{D}_{zz}^{(\text{cyl})} > 0, \quad (8)$$

$k = 14.6$ for $\text{Mn}_{12} \text{Ac}$. For other shapes such as elongated rectangular, one obtains qualitatively similar expressions.¹⁴ Now the total field is given by

$$B_{\text{tot},z}(z) = B_z + B_z^{(D)}(z) = B_z + \frac{Sg\mu_B}{v_0} D_{zz}(z). \quad (9)$$

One of the dynamical equations of the model is the relaxation equation for the metastable population $n(t, z)$

$$\frac{\partial n(t, z)}{\partial t} = -\Gamma(B_{\text{tot},z}(z), T(z)) \left[n(t, z) - n^{(\text{eq})}(T) \right]. \quad (10)$$

In Eq. (10) $\Gamma(\dots)$ is the relaxation rate taking into account both thermal activation over the barrier and resonance spin tunneling that is calculated from the density matrix equation. As $B_{\text{tot},z}$ depends on $n(z)$ everywhere in the sample via Eqs. (7) and (3), this is an integro-differential equation. In the sequel we will set $n^{(\text{eq})} \Rightarrow 0$ that is a good approximation for strong enough bias.²

The second equation is the heat conduction equation that is convenient to write in terms of the energy \mathcal{E} of the system per unit cell as in Ref. 2 In the full-burning case $n^{(\text{eq})} = 0$ this equation has the form

$$\frac{\partial \mathcal{E}(t, z)}{\partial t} = \frac{\partial}{\partial z} \kappa \frac{\partial \mathcal{E}(t, z)}{\partial z} - n_0 \Delta E \frac{\partial n(t, z)}{\partial t}. \quad (11)$$

In Eq. (11) κ is the thermal diffusivity and ΔE is the energy released in the transition of a spin from the metastable state to the ground state,

$$\Delta E = 4hDS^2, \quad h \equiv \frac{g\mu_B B_z}{2DS}. \quad (12)$$

The relation between the energy \mathcal{E} and temperature is given by $\mathcal{E}(T) = \int_0^T C(T')dT'$, where $C(T)$ is the experimentally measured heat capacity per unit cell.¹⁶

To solve the system of Eqs. (10) and (11) numerically, it is convenient to introduce reduced variables²

$$\tilde{\mathcal{E}} \equiv \frac{\mathcal{E}}{n_0 \Delta E}, \quad \tau \equiv t \Gamma_f, \quad \tilde{\mathbf{r}} \equiv \frac{\mathbf{r}}{l_d}, \quad (13)$$

where $n_0 \leq 1$ is the initial population of the metastable state and Γ_f is the relaxation rate at the flame temperature T_f defined by the energy balance $n_0 \Delta E = \mathcal{E}(T_f)$ and some fixed value of $B_{\text{tot},z}$ that we set to the resonance field B_k . The characteristic distance $l_d = \sqrt{\kappa_f / \Gamma_f}$ defines the width of the deflagration front in the case of normal (thermal) deflagration and κ_f is the thermal diffusivity at T_f . In terms of these variables, Eqs. (10) and (11) become

$$\frac{\partial \tilde{\mathcal{E}}}{\partial \tau} = \frac{\partial}{\partial \tilde{z}} \tilde{\kappa} \frac{\partial \tilde{\mathcal{E}}}{\partial \tilde{z}} - \frac{\partial n}{\partial \tau} \quad (14)$$

$$\frac{\partial n}{\partial \tau} = -\tilde{\Gamma} \left(B_{\text{tot},z}, T(\tilde{\mathcal{E}}) \right) n, \quad (15)$$

where $\tilde{\Gamma} \equiv \Gamma / \Gamma_f$ is the reduced relaxation rate and $\tilde{\kappa} \equiv \kappa / \kappa_f$. It remains to add the expression for $B_{\text{tot},z}$ in reduced variables, Eq. (9) with $D_{zz}(\tilde{z})$ given by Eq. (7) with $z \Rightarrow \tilde{z}$ and $R \Rightarrow \tilde{R} \equiv R / l_d$. The important parameter \tilde{R} is the ratio of the width of the front of tunneling that is of order R (see Refs. 13,14) to the width of the standard deflagration front l_d .^{2,9}

Eqs. (14) and (15) are solved numerically by choosing a finite-length sample and discretizing the problem in \tilde{z} . This yields a system of ordinary differential equations in time. We set $\tilde{\kappa} = 1$ for simplicity. Before solving the equations, $\tilde{\Gamma}$ was calculated from the density matrix equation⁶ for the transverse field $B_{\perp} = 3$ T and tabulated as a function of $B_{\text{tot},z}$ and \mathcal{E} . As $\tilde{\Gamma}$ increases by many orders of magnitude near tunneling resonances, one has to use many different values of $B_{\text{tot},z}$ for interpolation here. In Fig. 2 one can see that for such a strong transverse field the barrier is reduced to zero at resonance where Γ practically does not depend of temperature. Thus near the resonance the cold deflagration should dominate, while off resonance the regular deflagration should take place.

For the discussion it is convenient to consider the energy bias $W = \varepsilon_{-S} - \varepsilon_{m'}$ between the two resonant levels,

$$W = (S + m') g \mu_B \left(B_z + B_z^{(D)} - B_k \right) \equiv W_{\text{ext}} + W^{(D)}. \quad (16)$$

It is convenient to use the reduced external bias

$$\tilde{W}_{\text{ext}} \equiv \frac{W_{\text{ext}}}{2E_D} = \left(1 + \frac{m'}{S} \right) \frac{v_0}{2Sg\mu_B} (B_z - B_k), \quad (17)$$

where $E_D \equiv (Sg\mu_B)^2 / v_0$ is the dipolar energy, $E_D / k_B = 0.0671$ K for Mn_{12} Ac. At the right end of the dipolar window of Eq. (1) one has $B_z = B_k + B^{(D)}$. Thus with the help of Eq. (4) one obtains $\tilde{W}_{\text{ext}} = (1/2) (1 + m'/S) D_{zz}$,

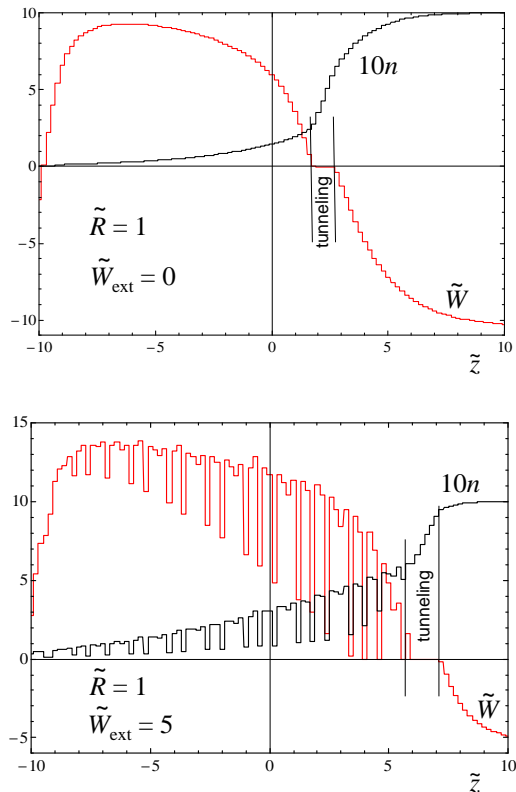


FIG. 3: Profiles of the metastable population n and the total bias \tilde{W} across the front for two values of the external bias \tilde{W}_{ext} : (a) $\tilde{W}_{\text{ext}} = 0$, laminar regime; (b) $\tilde{W}_{\text{ext}} = 5$, non-laminar regime

i.e., $\tilde{W}_{\text{ext}} \approx D_{zz}$ for small bias, $m' \approx S$. We will see that in the case of strong tunneling the speed of the quantum deflagration front has a maximum at the right end of the dipolar window, $\tilde{W}_{\text{ext}} \approx \bar{D}_{zz}^{(\text{cyl})} = 10.53$ for Mn_{12} Ac.

Cold deflagration can be ignited by the field sweep across the resonance. In this case ignition occurs around the „magic“ value $\tilde{W}_{\text{ext}} \cong 5$ that corresponds to $B_z - B_k \cong 22$ mT.^{13,14} Outside the dipolar window fronts of tunneling do not exist. On the other hand, standard deflagration can be initiated, at any bias, by a quick temperature rise on one side of the sample.² Applying this method of ignition here, we will see that within the dipolar window the process is modified by spin tunneling and the speed of the burning front can significantly increase for $\tilde{R} \gtrsim 1$, especially at the right end of the window.

There are two regimes of propagation of non-thermal fronts of tunneling: Laminar and non-laminar. Laminar regime with a smooth front takes place in the left part of the dipolar window, $0 \leq B_z - B_k \leq 10$ mT (or $0 \leq \tilde{W}_{\text{ext}} \leq 1.3$), while the non-laminar regime with frozen-in quasiperiodic spatial patterns of the magnetization behind the front is realized in the right part of the dipolar window. In both regimes burning is not complete and becomes less complete with increasing the bias. In the laminar regime the residual magnetization and

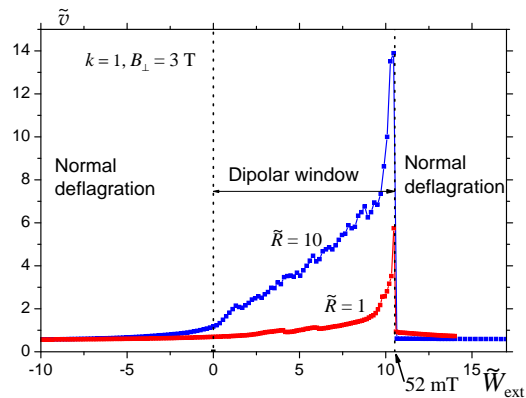


FIG. 4: Reduced front speed \tilde{v} vs bias field for different values of the reduced transverse size $\tilde{R} \equiv R/l_d$, l_d being the width of the thermal deflagration front. For such a strong applied transverse field, the effect of tunneling is dramatic.

the front speed were calculated analytically.¹⁴ The front speed increases with the bias. In the non-laminar regime, quasi-periodic frozen-in patterns of magnetization deteriorate the resonance condition, and the front speed decreases with the bias after the breakdown of the laminar regime (see Fig. 5 of Ref. 14). Thermal mechanism of deflagration leads to complete burning of this residual metastable population that smoothens the dipolar field profile in the sample and improves the resonance condition inside the front core. This leads to the increase of the front speed because of spin tunneling in the whole dipolar window.

Results of numerical calculations for the spatial profiles of the metastable population n and the total bias

\tilde{W} in the front for $\tilde{R} = 1$ are shown in Fig. 3. Both in the laminar and non-laminar regimes, there is a region where $\tilde{W} \cong 0$ and resonant tunneling takes place, causing a greater slope of $n(z)$. Behind the front (on the left) metastable population n burns to zero via thermal mechanism.

Numerical solutions for the reduced front speed $\tilde{v} = v/(l_d\Gamma_f)$ (Ref. 11) for the generic model with $B_\perp = 3$ T and $\tilde{R} = 1$ and 10 are shown in Fig. 4. Within the dipolar window the front speed can largely exceed the speed of regular deflagration and depends on the transverse crystal size R parametrized by \tilde{R} . At $B_\perp = 3$ T the maximal values of \tilde{v} are attained at the right end of the dipolar window, followed by a steep drop towards the standard-deflagration result outside the dipolar window. For smaller transverse fields such as 2 T, the effect of spin tunneling is weaker and \tilde{v} reaches a maximum somewhere in the middle of the dipolar window, depending on \tilde{R} .

Measurements of the speed of deflagration fronts^{9,10} were done in zero or small transverse field, so that the influence of resonance spin tunneling on the front speed is not so dramatic as in Fig. 4. It would be highly interesting to perform deflagration experiments in strong enough transverse field to see the big effect of tunneling on the front propagation. Changing thermal contact of the crystal with the environment, one can boost or suppress the thermal mechanism of magnetic burning thus isolating thermal and quantum effects from each other.

Numerous useful discussions with E. M. Chudnovsky are gratefully acknowledged.

This work has been supported by the NSF Grant No. DMR-0703639.

¹ J. R. Friedman, M. P. Sarachik, J. Tejada, and R. Ziolo, Phys. Rev. Lett. **76**, 3830 (1996).
² D. A. Garanin and E. M. Chudnovsky, Phys. Rev. B **56**, 11102 (1997).
³ E. M. Chudnovsky and D. A. Garanin, Phys. Rev. Lett. **79**, 4469 (1997).
⁴ D. A. Garanin, X. M. Hidalgo, and E. M. Chudnovsky, Phys. Rev. B **57**, 13639 (1998).
⁵ D. A. Garanin and E. M. Chudnovsky, Phys. Rev. B **59**, 3671 (1999).
⁶ D. A. Garanin, arXiv:0805.0391 (2008).
⁷ E. M. Chudnovsky, Phys. Rev. Lett. **92**, 120405 (2004).
⁸ E. M. Chudnovsky, D. A. Garanin, and R. Schilling, Phys. Rev. B **72**, 094426 (2005).
⁹ Y. Suzuki, M. P. Sarachik, E. M. Chudnovsky, S. McHugh, R. Gonzalez-Rubio, N. Avraham, Y. Myasoedov, E. Zeldov, H. Shtrikman, N. E. Chakov and G. Christou, Phys.

Rev. Lett. **95**, 147201 (2005).
¹⁰ A. Hernández-Minguez, J. M. Hernández, F. Macia, A. Garcia-Santiago, J. Tejada, P. V. Santos, Phys. Rev. Lett. **95**, 217205 (2005).
¹¹ D. A. Garanin and E. M. Chudnovsky, Phys. Rev. B **76**, 054410 (2007).
¹² D. A. Garanin and E. M. Chudnovsky, Phys. Rev. B **78**, 174425 (2008).
¹³ D. A. Garanin and E. M. Chudnovsky, Phys. Rev. Lett. **102**, 097206 (2009).
¹⁴ D. A. Garanin, Phys. Rev. B **80**, 014406 (2009).
¹⁵ S. McHugh, R. Jaafar, M. P. Sarachik, Y. Myasoedov, H. Shtrikman, E. Zeldov, R. Bagai, and G. Christou, Phys. Rev. B **79**, 052404 (2009).
¹⁶ A. M. Gomes, M. A. Novak, R. Sessoli, A. Caneschi, and D. Gatteschi, Phys. Rev. B **57**, 5021 (1998).